Dynamics of the Optimal State for Cold Pools in Shear

George H. Bryan and Richard Rotunno
National Center for Atmospheric Research

1. Background:

- This study revisits the "optimal state" for gravity currents in sheared environments, which was first hypothesized by Rotunno et al. (1988) (hereafter RKW).

- Conceptual model (Fig. 1): a sheared environmental flow is turned into a vertically oriented jet at the leading edge of a cold pool.

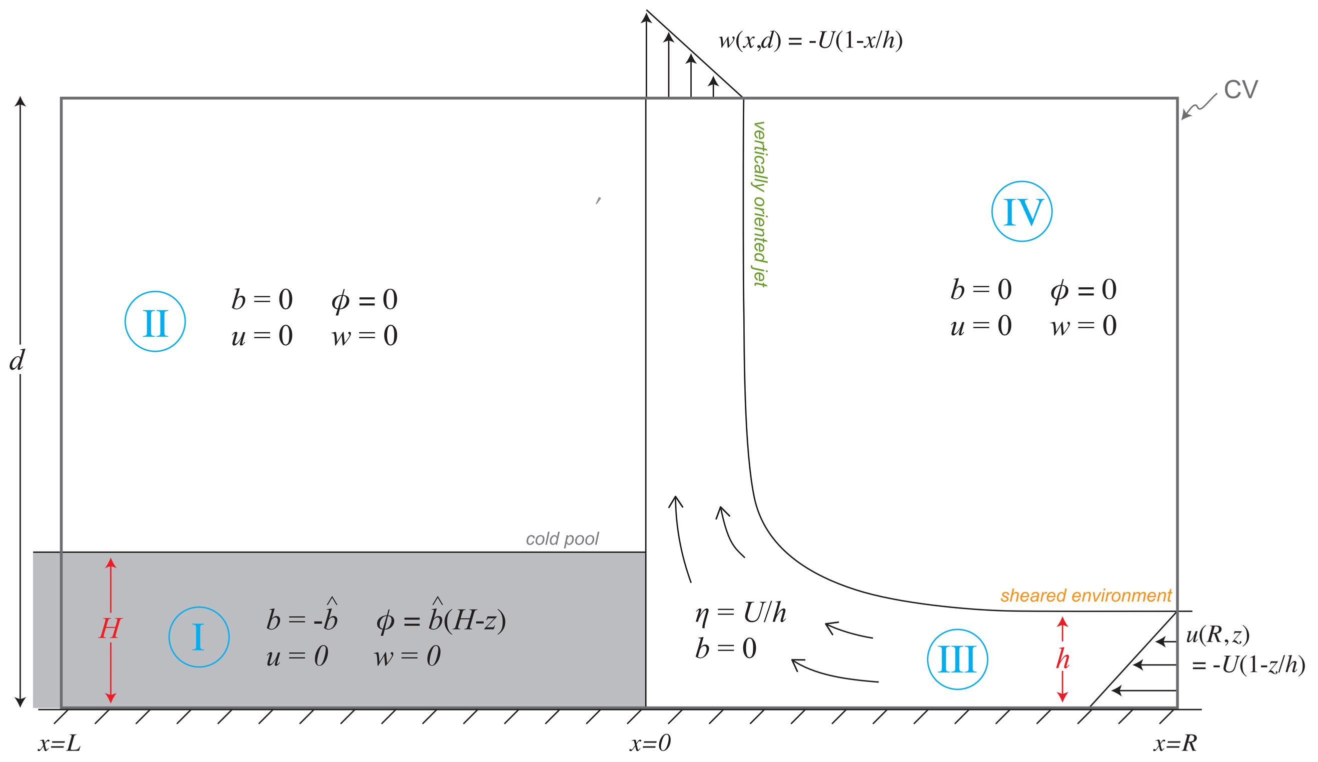

Fig. 1: Idealized schematic of the optimal state for a gravity current in a sheared environment.

H: depth of the cold pool
h: depth of the environmental shear layer

Region I: a stagnant (relative to surface gust front) cold pool of constant potential temperature deficit
Region II: a neutral, stagnant (relative to surface gust front) layer directly over the cold pool
Region III: a neutral layer of constant positive vorticity, entering from the right side, and deflected upward
Region IV: a neutral, stagnant (relative to surface gust front) zone bounding the constant-vorticity layer

- This overall structure is referred to as "the optimal state," a term chosen by RKW to highlight the fact that lifting of environmental air is maximized (i.e., optimized) in this configuration.

2. Control Volume Constraints

- We perform Control Volume (CV) analyses on the flow in Fig. 1.

- Assumptions: steady, viscous flow; free slip lower boundary.

- See Bryan and Rotunno (2013) for governing equations, further assumptions, and additional details.

- Result from vorticity balance: $U = (2\hat{b}H)^{1/2}$ (1)

  - Interpretation: the import of positive vorticity associated with environmental shear [left side of (1)] equals the net buoyant generation of vorticity within the CV [right side of (1)].
  - (1) is the same as RKW's Eqn. (10); here we clarify that this result is also valid for viscous flow.
  - Left side of (1) [i.e., U] also quantifies the wind difference over depth h and is often represented as Δu.
  - Right side of (1) also quantifies the "intensity" of a cold pool and is often represented simply as c.
  - Note: (1) was derived assuming a linear profile of $u(z)$; the same result arises from any form of $u(z)$.

- Result from flow-force (i.e., momentum) balance: $h/H = 3/4$ (2)

  - Interpretation: the column-integrated hydrostatic pressure in the cold pool must match the column-integrated horizontal momentum flux; in other words, the incoming (horizontal) momentum is "stopped" by the cold pool.
  - (2) is a previously unpublished constraint on the shear-layer depth h (relative to cold-pool depth H).
  - Note: (2) is specific to an assumed linear profile of $u(z)$; other forms of $u(z)$ yield different constraints for h/H (see Bryan and Rotunno, 2013, §6).

3. Interior Solution for Steady Inviscid Flow

- Assuming steady, inviscid, and adiabatic flow, we obtain a unique solution for the outflow profile $w(x,d)$ [top-center of Fig. 1].

- Then we determine the shape of the free boundary between Regions I and III, and thus the entire interior flow (Fig. 2).

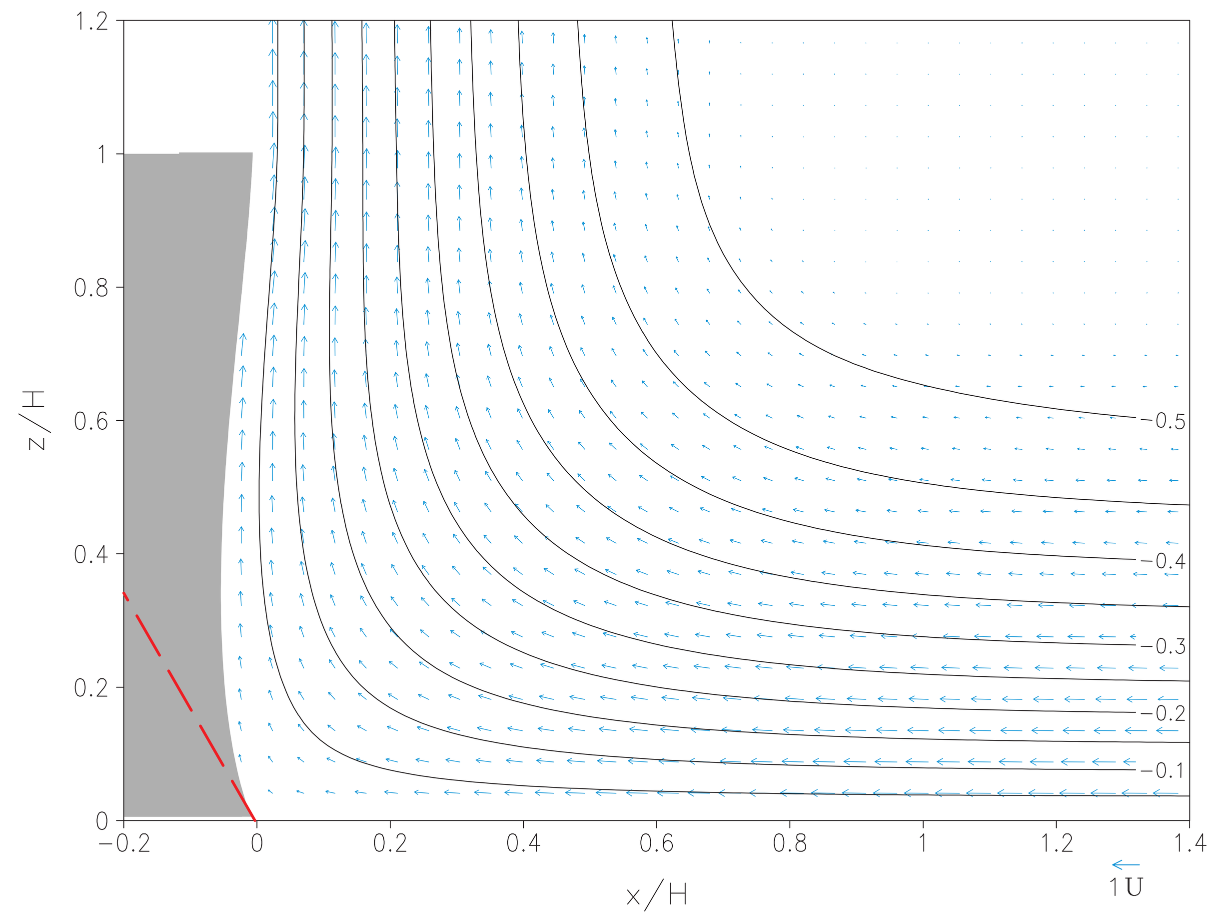

Fig. 2: Numerical solution for the optimal state assuming steady, inviscid, adiabatic flow. Gray shading denotes the cold pool, black contours show streamfunction ψ (contour interval 0.05), and flow vectors are shown every fourth gridpoint. The red-dashed line indicates a 60° angle from the horizontal [Rottman et al. (1985), Xu (1992)].

- The leading edge of the cold pool is slightly concave, but is predominantly vertical.

- The flow hypothesized by RKW satisfies the steady, inviscid, adiabatic equations of motion everywhere.

4. Time-Dependent Numerical Simulations

- Direct Numerical Simulations; initialized with CV constraints (1) and (2).

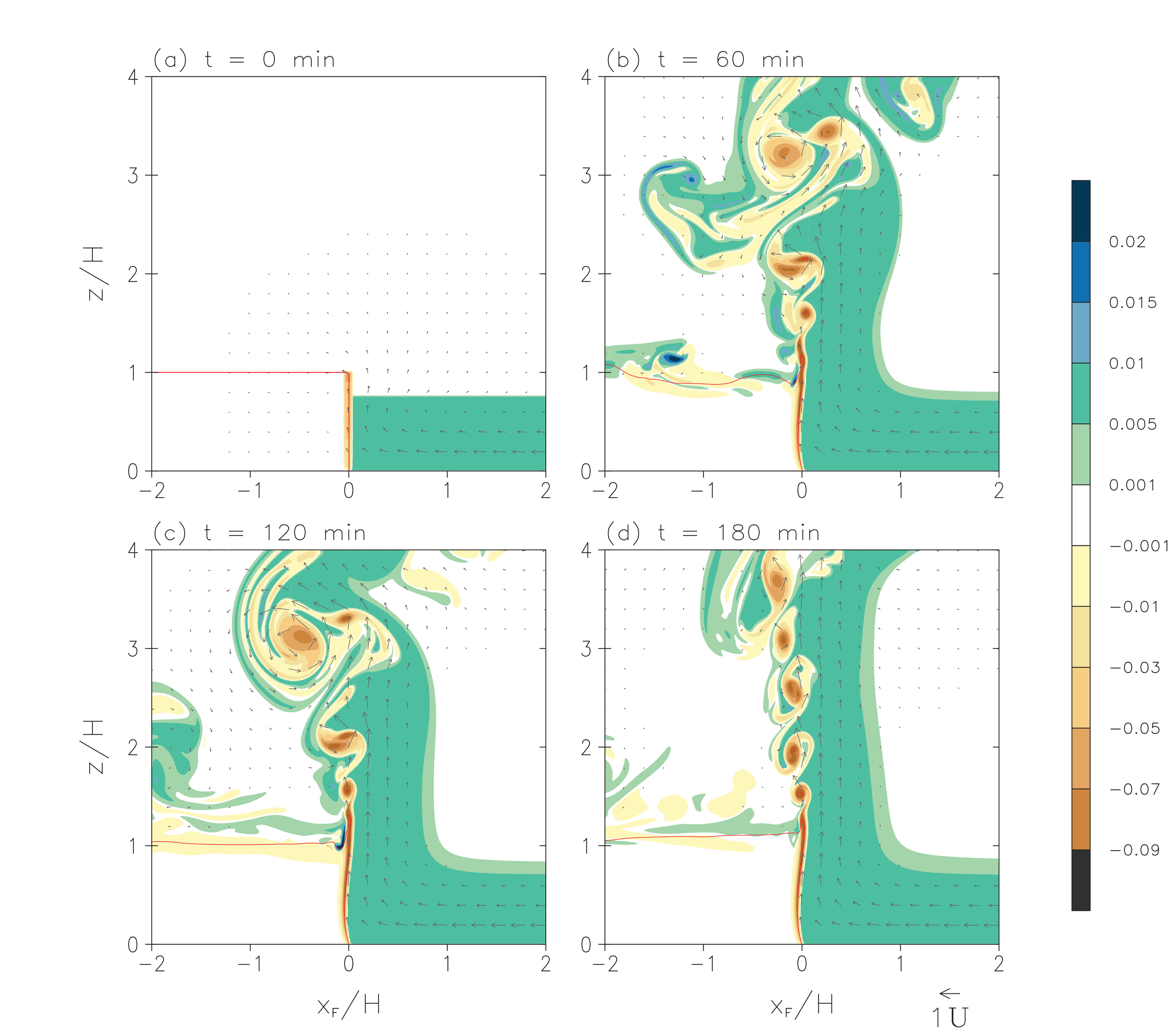

Fig. 3: Instantaneous snapshots from a numerical simulation at t = (a) 0, (b) 60, (c) 120, and (d) 180 min. Gray flow vectors are shown every 16th grid point (vectors with a magnitude less than $0.05U$ are excluded). The red contour shows nondimensional buoyancy $b = 0.5$. Color shading is vorticity.

5. Comparison of Simulation and Theory

- A vertically oriented jet emerges in the simulation and remains statistically steady (Fig. 3); transient eddies develop on the left side.

- All the important elements of the theoretical flow (Fig. 1) are seen in the numerical solution (Fig. 3), e.g.: the front-relative flow remains negligible behind the surface gust front ($x_F < 0$) at all levels; and the leading edge of the cold pool is predominantly vertical.

- Vorticity budget:

$$0 = \underbrace{-\frac{\partial}{\partial t}\int_L^R\int_0^d \eta\,dx\,dz}_{\text{tendency}} + \underbrace{\int_0^d (u\eta)_L\,dz}_{\text{flux at left}} - \underbrace{\int_0^d (u\eta)_R\,dz}_{\text{flux at right}} - \underbrace{\int_L^R (w\eta)_d\,dz}_{\text{flux at top}} + \underbrace{\int_0^d (B_L - B_R)\,dz}_{\text{net generation}}, \quad (3)$$

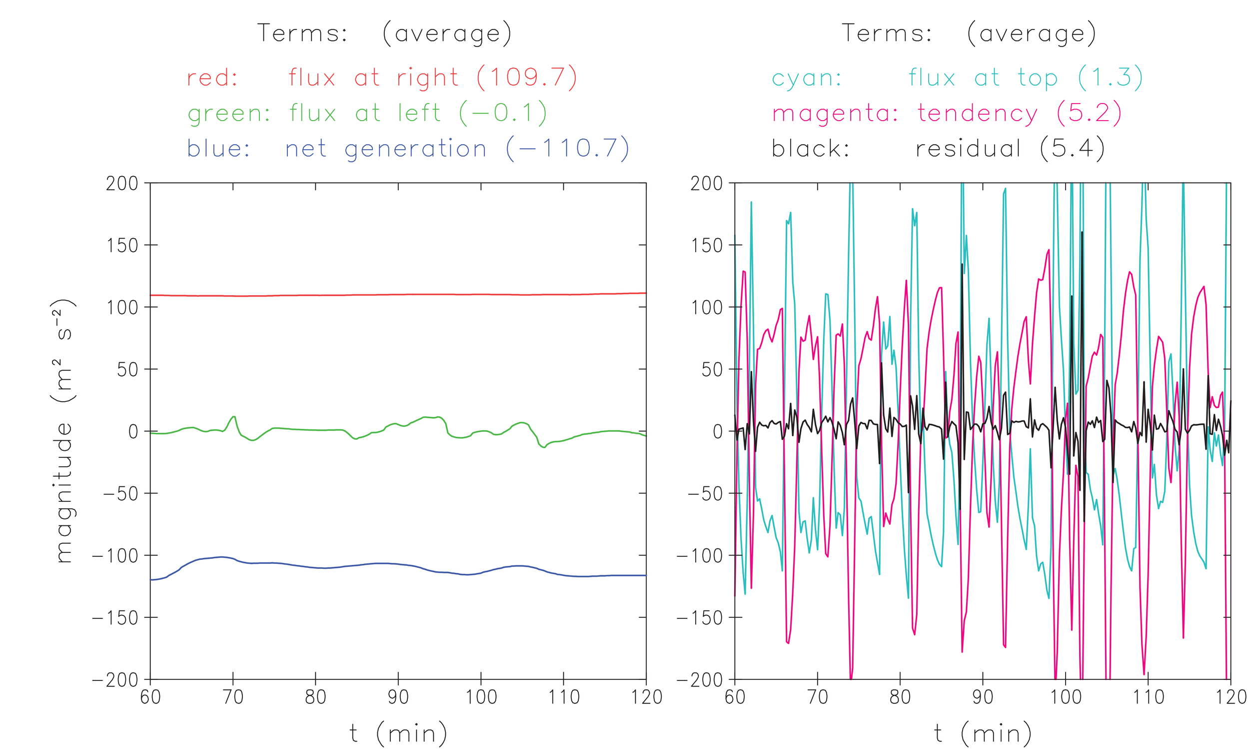

Fig. 4: Time evolution of terms in the horizontal vorticity budget, as indicated by the legend at the top [corresponding to terms in (3)]. Numbers in parentheses in the legend denote the average value over this time period. The control volume for this analysis is $-2 \le x_F/H \le +2$ and $0 \le z/H \le 2$.

- As hypothesized by RKW, the "flux at right" term (red) closely matches the "net generation" term (blue) and the "flux at left" term (green) is negligible. Other terms oscillate about zero.

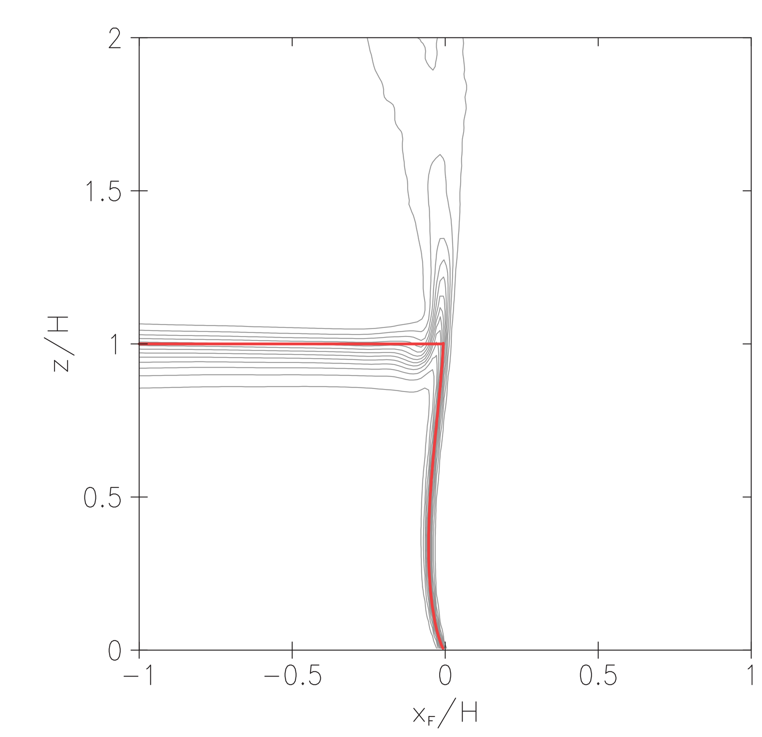

Fig. 5: Comparison of the theoretical interface for steady, inviscid, isentropic flow (red curve from Section 3) with time-averaged potential temperature from the numerical simulation (gray contours).

- The only major difference is that negatively buoyant air that is drawn upward in the simulation (partly because of viscosity and conductivity in the numerical model).

Acknowledgments:

The National Center for Atmospheric Research is sponsored by the National Science Foundation.

The authors thank the Computational and Information Systems Laboratory (CISL) of NCAR for providing MUDPACK, the multigrid software for elliptic equations that was used in this study.

The authors also acknowledge high-performance computing support from Yellowstone (ark:/85065/d7wd3xhc), provided by NCAR/CISL, and sponsored by the National Science Foundation.

References

Bryan, G. H., and R. Rotunno, 2013: The optimal state for gravity currents in shear. Submitted to *J. Atmos. Sci.* [available at http://www.mmm.ucar.edu/people/bryan/]

Rottman, J. W., J. C. R. Hunt, and A. Mercer, 1985: The initial and gravity-spreading phases of heavy gas dispersion: Comparison of models with Phase I data. *J. Hazardous Materials,* **11,** 261–279.

Rotunno, R., J. B. Klemp, and M. L. Weisman, 1988: A theory for strong, long-lived squall lines. *J. Atmos. Sci.,* **45,** 463–485.

Xu, Q., 1992: Density currents in shear flows – A two-fluid model. *J. Atmos. Sci.,* **49,** 511–524.

 Corresponding author: George H. Bryan, e-mail: gbryan@ucar.edu